Template-Directed Self-Assembly and Growth of Insulin Amyloid Fibrils

Chanki Ha, Chan Beum Park

Department of Chemical and Materials Engineering & Science and Engineering of Materials Program, Arizona State University, Tempe, Arizona 85287; telephone: +1 (480) 965-0362; fax: +1 (480) 965-0037; e-mail: cbpark@asu.edu

Received 1 December 2004; accepted 27 January 2005

Published online 31 March 2005 in Wiley InterScience (www.interscience.wiley.com). DOI: 10.1002/bit.20486

Abstract: The formation of amyloid aggregates in tissue is a pathological feature of many neurodegenerative diseases and type II diabetes. Amyloid deposition, the process of amyloid growth by the association of individual soluble amyloid molecules with a pre-existing amyloid template (i.e., plaque), is known to be critical for amyloid formation in vivo. The requirement for a natural amyloid template, however, has made amyloid deposition study difficult and cumbersome. In the present work, we developed a novel, synthetic amyloid template by attaching amyloid seeds covalently onto an *N*-hydroxysuccinimide-activated surface, where insulin was chosen as a model amyloidogenic protein. According to ex situ atomic force microscopy observations, insulin monomers in solution were deposited onto the synthetic amyloid template to form fibrils, like hair growth. The fibril formation on the template occurred without lag time, and its rate was highly accelerated than in the solution. The fibrils were long, over 2 μm, and much thinner than those in the solution, which was caused by limited nucleation sites on the template surface and lack of lateral twisting between fibrils. According to our investigations using thioflavin T-induced fluorescence, birefringent Congo red binding, and circular dichroism, fibrils grown on the template were identified to be amyloids that formed through a conformational rearrangement of insulin monomers upon interaction with the template. The amyloid deposition rate followed saturation kinetics with respect to insulin concentration in the solution. The characteristics of amyloid deposition on the synthetic template were in agreement with previous studies performed with human amyloid plaques. It is demonstrated that the synthetic amyloid template can be used for the screening of inhibitors on amyloid deposition in vitro. © 2005 Wiley Periodicals, Inc.

Keywords: amyloid deposition; synthetic amyloid template; plaque growth; insulin; self-assembly; drug screening; neurodegenerative diseases

INTRODUCTION

Protein misfolding and aggregation pose critical problems in human medicine and biotechnology (Macario and de Macario, 2000; Slavotinek and Biesecker, 2001; Thomas et al., 1995). In particular, the formation of amyloid aggregates in tissues is a pathological feature of many diseases, such as Alzheimer's, Parkinson's, Huntington's, mad cow disease and type II diabetes (Harper and Lansbury, 1997; Murphy, 2002). Amyloid, the term first introduced by the German physician Rudolph Virchow in 1854, refers to protein aggregates having several physicochemical features in common: a fibrillar morphology, a predominantly cross β-sheet secondary structure, birefringence upon staining with Congo red dye, and insolubility in an aqueous solution (Murphy, 2002; Sipe and Cohen, 2000). Due to the possible relation of amyloid to pathology (Rochet and Lansbury, 2000; Wang et al., 2002), many efforts had been made to screen compounds that interfere with amyloid formation in vitro (Conway et al., 2001; Tjernberg et al., 1996; Tomiyama et al., 1996). Under various destabilizing conditions, amyloidogenic protein undergoes an alternate folding pathway and interacts to form fibrillar aggregates (Ahmad et al., 2003; Fändrich et al., 2001; Harper and Lansbury, 1997; McLaurin et al., 2000). For over a century, it still remains unresolved how normal and soluble proteins assemble into fibrillar and insoluble aggregates (Kisilevsky, 2000).

The key to understanding the underlying etiology of amyloid diseases lies in careful examination of amyloid aggregation and the environmental conditions that induce normal protein to undergo pathogenic fibrillation (Kisilevsky, 2000; Lansbury, 1999; Serpell, 2000). Amyloid formation in tissues takes place dominantly in the proximity of membranes, and its rate is highly accelerated in the presence of preformed plaques (Kowalewski and Holtzman, 1999; Sharp et al., 2002; Zhu et al., 2002). Increasing evidence shows that the interaction of soluble amyloid monomers with a solid surface is critical for amyloid formation in vivo. Esler et al. (2000) modeled the process of Alzheimer's amyloid plaque growth by monitoring the deposition of radiolabeled amyloid-β monomers onto human plaque, and they found that the transition from monomer to neurotoxic amyloid was mediated by interaction with the plaque. A similar phenomenon was also observed in the conformational rearrangement and aggregation of prion protein, the normal cell-surface component of neurons, which is implicated with mad cow and Creutzfeld–Jacob disease (Cohen and Prusiner, 1998; Rymer and Good, 2000). The mechanism underlying the amyloid formation of an

Correspondence to: C. B. Park

© 2005 Wiley Periodicals, Inc.

immunoglobulin light chain on a mica surface was significantly different from that in the solution, which was believed to be more physiologically relevant (Zhu et al., 2002).

Despite the apparent role of amyloid deposition in amyloidosis, however, the requirement for tissue plaque and its centrifugation made the study difficult and cumbersome. The difficulties associated with a ''natural'' amyloid template recently led to the development of an ''artificial'' template. Esler et al. (1997, 1999) developed a synthetic amyloid template by adding an aliquot of an amyloid-β solution into a 96-well assay plate followed by drying the plate overnight. The plate, each well of which was physically coated with preformed amyloids, was then incubated in radiolabeled amyloid-β monomer solution for the subsequent study of amyloid deposition onto the template under different environmental conditions. The synthetic amyloid template was found to be indistinguishable from plaques in an Alzheimer's disease patient. However, the amyloid seeds and fibrils formed on the template were unstable due to the weak nature of physical adsorption. Fibril growth on the template could not be observed visually, and amyloid-β monomers in the solution should be radiolabeled before incubation for quantitative analysis of the deposition.

In the present study, we developed a novel, synthetic amyloid template suitable for amyloid deposition study in vitro. The template, prepared by attaching amyloid seeds covalently onto a chemically derivatized glass surface, was found to be highly stable. The fibril growth on the template could be analyzed directly using multiple tools that include ex situ atomic force microscopy, thioflavin T-induced fluorescence, birefringent Congo red binding, and circular dichroism. Insulin was chosen here as a model amyloidogenic protein, which had been known to form amyloid fibrils under various destabilizing conditions in vitro (Ahmad et al., 2003; Bouchard et al., 2000; Nielsen et al., 2001). Amyloid deposits of insulin had been observed both in patients with type II diabetes as well as after insulin infusion and repeated injection (Ahmad et al., 2003; Brange et al., 1997). According to our work, insulin monomers present in the solution associated rapidly onto a seeded template to grow like hair. Compatible solutes, such as sucrose, maltose, trehalose, and betaine, were tested to demonstrate the possibility of using the template for a high-throughput screening of inhibitors on amyloid deposition. By using the synthetic amyloid template developed in this work, amyloid deposition for other amyloidogenic proteins can be modeled readily in vitro.

MATERIALS AND METHODS

Materials

Bovine insulin, 3-aminopropyltriethoxysilane (APTS),*N,N*′-disuccinimidyl carbonate (DSC), 2-mercaptoethanol, *N,N*-dimethylformamide (DMF), bovine serum albumin, thioflavin T (ThT), and Congo red (CR) were purchased from Sigma-Aldrich (St. Louis, MO). Micro cover glasses were obtained from VWR Scientific (West Chester, PA).

Preparation of *N*-Hydroxysuccinimide (NHS)-Activated Surface

Micro cover glasses were chemically derivatized to mediate covalent attachments of the insulin amyloid seeds. Glass slides were cleaned in a piranha solution of 70% H_2SO_4: 30% H_2O_2 (7:3, v/v) for 12 h at room temperature followed by rinsing with deionized water. The slides were then treated with a 3% solution of APTS in ethanol/water (95:5, v/v) for 1 h, dipped in 100% ethanol, and cured at 110°C for 1 h. After cooling and washing with 95% ethanol, the slides were treated with 20 mM DSC solution in a sodium bicarbonate buffer (50 mM, pH 8.5) for 3 h, followed by washing with deionized water and drying with N_2.

Deposition on Synthetic Amyloid Template

The solution of bovine insulin at 1 mg/mL in an HCl solution (40 mM) was pre-incubated at 50°C for 6 h to prepare the amyloid seeds for immobilization. A 20-μL aliquot from the solution was then introduced uniformly onto the entire surface of an NHS-activated glass slide. The template with the covalently bonded amyloid seeds was then put into a 2-mercaptoethanol/DMF solution (1:99, v/v) for 45 min, washed with deionized water for 1 h, and dried with N_2. We tested the effect of the 2-mercaptoethanol/DMF solution on the amyloid seeds by comparing it with the bovine serum albumin solution (0.1% wt) and the phosphate buffer (50 mM, pH 7.4), respectively. It was found that the treatment with 2-mercaptoethanol/DMF did not affect the insulin fibril growth on the template (data not shown). Template-directed fibril growth was made by incubating the synthetic amyloid template in a fresh insulin solution of 1 mg/mL in HCl solution (40 mM) at 50°C. After incubation, the substrate was washed with DMF, deionized water, and dried with N_2 for further analysis.

Ex Situ Atomic Force Microscopy (AFM)

Fibril growth on a synthetic amyloid template (8 mm × 8 mm) was visualized with et situ AFM without the use of mica. For the analysis of insulin in the solution phase, a 5-μL aliquot of insulin solution was placed on freshly cleaved mica at room temperature. AFM tips were used at a resonant frequency of 306–444 kHz for imaging fibrils with a Nanoprobe III scanning probe workstation (Digital Instruments Inc., Fremont, CA). Images were acquired in a tapping mode under ambient conditions at a scan frequency of 1–2 Hz. Height distribution analysis was carried out with SPIP software (Image Metrology A/S, Lyngby, Denmark). At least two different samples and five spots with an area of 2 × 2 μm were analyzed in each case. Representative images were selected for comparative studies.

Thioflavin T (ThT)-induced Fluorescence

ThT stock solution was prepared at 500 μM in a Tris-HCl buffer (pH 8, 20 mM) and was filtered through a nylon sterile

filter (0.2-μm pore size) before use. The template samples (8 mm × 18 mm) deposited with the insulin amyloid fibrils were put diagonally into a 10-mm path-length quartz cuvette containing 2 mL of 50-μM ThT solution. Fluorescence measurements were performed with a spectrofluorometer (Model RF5301, Shimadzu Co., Japan).

Circular Dichroism (CD)

CD spectra of insulin samples were measured on a spectropolarimeter (Model J-710, Jasco Co., Tokyo, Japan) from 190 to 260 nm at a scan speed of 50 nm/min and resolution of 0.5 nm. The CD spectra were recorded using a 0.1-mm path-length quartz cell for insulin aggregates grown in the solution and a 10-mm path-length quartz cuvette for insulin deposited on the template (8 mm × 18 mm), respectively.

Birefringent Congo Red (CR) Binding

CR solution was prepared at 25 μM of concentration in a Tris-HCl buffer (pH 8, 20 mM) containing 10% ethanol, which was filtered through a nylon sterile filter (0.2-μm pore size) before use. The template samples (8 mm × 18 mm) deposited with the insulin amyloid fibrils were put into the CR solution for 10 min at room temperature, followed by washing with deionized water. The template samples were then placed diagonally in a quartz cuvette (10-mm path-length) containing a Tris-HCl buffer (pH 8, 20 mM). Absorbance spectra were measured from 400 to 700 nm with a spectrophotometer (Shimadzu Co., Japan).

RESULTS AND DISCUSSION

Template-Directed Growth of Insulin Fibrils

In order to investigate amyloid deposition onto a synthetic template, insulin amyloid seeds were covalently immobilized onto an NHS-activated surface. The seeds were obtained by incubating a fresh insulin solution for 6 h until the end of the lag phase in amyloid formation according to ThT-induced fluorescence analysis (data not shown). There was no visible amyloid fibril in the seed solution according to AFM analysis. After incubation of the template in a fresh insulin solution for 5 h, numerous insulin fibrils were observed on the template surface (Fig. 1A). In contrast, no fibrils were found in the solution phase where the seeded template was immersed and incubated (Fig. 1B). This phenomenon indicates that all the fibrils found on the template were formed by the deposition of insulin monomers in the solution onto the template surface.

The rate of fibril formation was highly accelerated by growing fibrils on the synthetic template. Amyloid fibrils were not found in the insulin solution over 10 h of incubation, while dense fibrils were seen on the template even after 1 h of incubation (data not shown). The rapid growth of amyloid fibrils on a surface was reported in a previous study where acceleration of amyloid fibril growth on a mica surface was observed for immunoglobulin light chains (Zhu et al., 2002). When a ''plain'' glass slide was tested instead of the activated slide to see the effect of chemical activation, few fibrils were found on the glass surface after 5 h of incubation (Fig. 1C). This shows that covalent immobilization is a more effective way than physical adsorption for growing amyloid fibrils on a solid surface. The height distribution of amyloid aggregates on the template was examined for AFM images of 0- and 5-h samples, respectively (Fig. 2). At 0 h, small oligomers (4.32 nm in mean height) were dominantly distributed with a Gaussian curve, whereas there was a substantial shift of aggregate size distribution (10.47 nm in mean height) after 5 h of incubation, which indicates the formation of insulin amyloid fibrils on the template.

Morphology of Insulin Fibrils Grown on Template

The morphology of fibrils grown on the synthetic template was significantly different from that formed in the solution. The majority of thin, twisted fibrils produced on the template had a faintly discernible cross-over repeat and a uniform size of over 2 μm in length (Fig. 1A), whereas distinct ropelike shapes of short and thick fibrils (Fig. 1D) were found when fibrils were formed in the solution without the template. According to previous reports, the thicker fibrils found in the solution resulted from association and twisting of a number of amyloid fibrils in vitro (Bouchard et al., 2000; Jiménez et al., 2002). The thin amyloid fibrils formed on the template indicate that lateral association of fibrils was suppressed by tight binding of the fibrils to the template surface. When the final length of fibrils was monitored, the template-directed fibrils were much longer than the fibrils grown in the solution in spite of a significantly shorter incubation time. The final length of amyloid fibril was known to be inversely proportional to the number of nuclei formed (Lomakin et al., 1996). In the case of the template-directed fibrillation, fibril length is expected to be longer because nucleation sites were confined only to the template surface by the attachment of seeds.

Characterization of Insulin Fibrils Grown on Template

The fibrils grown on the synthetic template were further characterized with ThT, CR, and CD analysis. ThT had been known to associate rapidly with amyloid aggregates, giving rise to a new emission maximum of around 485 nm (LeVine, 1993). Figure 3A shows a substantial increase of ThT-induced fluorescence for fibrils grown on the synthetic template, especially at around 485 nm. The increase of ThT fluorescence indicates self-assembly of native insulin monomers in the solution into amyloid fibrils on the template. The presence of ''amyloid'' fibrils on the template was also confirmed by an increased absorbance upon binding of CR to the fibrils (Fig. 3B). The evolution of a secondary structure during insulin deposition on the template was observed with CD spectra analysis (Fig. 4). The two maxima of negative

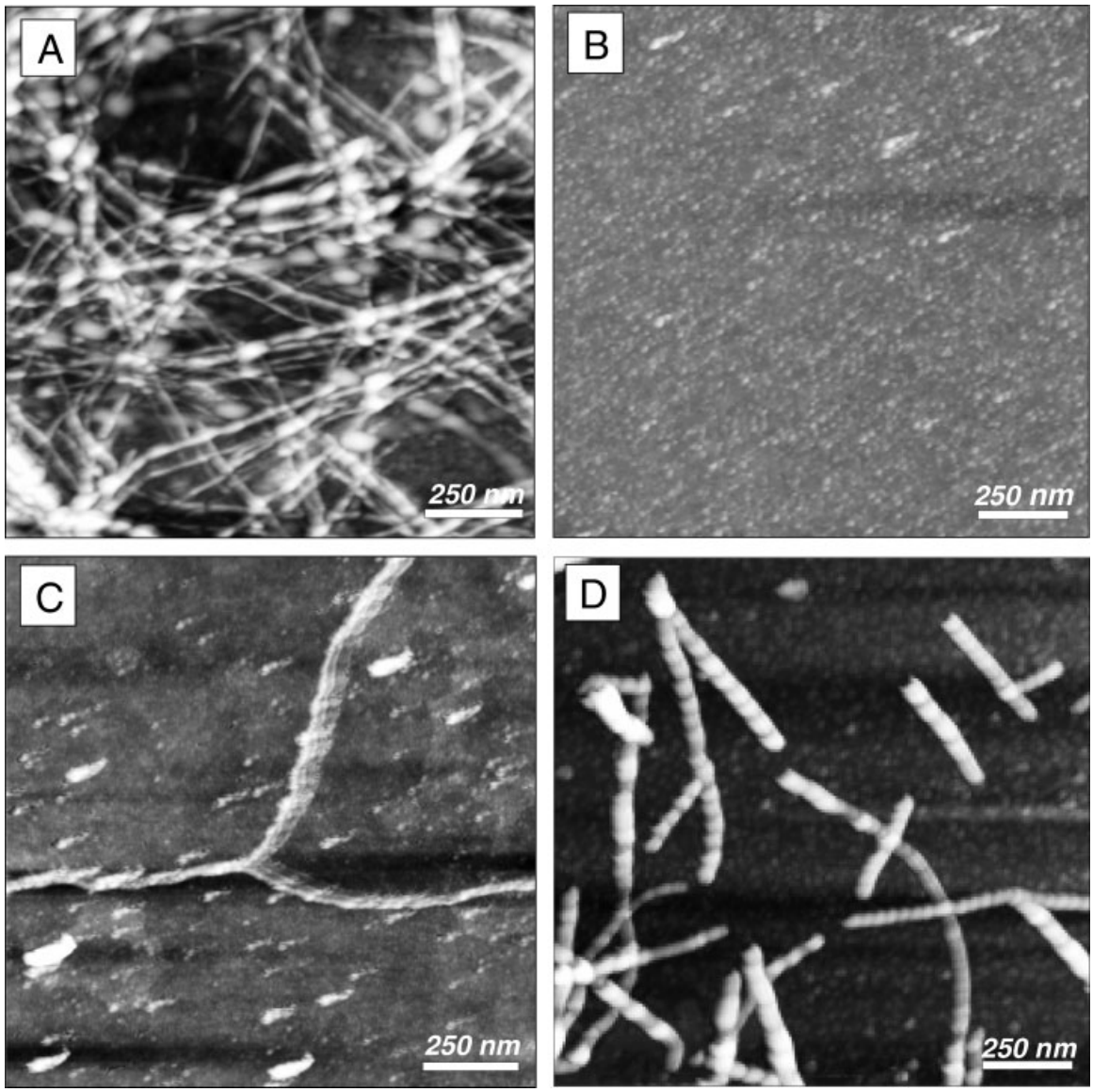

Figure 1. Representative AFM images of insulin samples prepared under different conditions. (**A**) Fibrils grown on the synthetic amyloid template for 5 h. (**B**) Insulin in the solution phase where the template was incubated for 5 h. (**C**) Fibrils grown on a plain glass slide with physically adsorbed seeds for 5 h. (**D**) Fibrils grown in a template-free solution for 24 h. All the incubations were performed with 1 mg/mL insulin solution in a capped glass vial.

ellipticity at 208 and 222 nm, indicating α-helical structure in native insulin decreased with the progress of incubation, and they were replaced by minimum at 216 nm indicating conformational change for fibrils grown on the template (Fig. 4A) as well as for those in the solution (Fig. 4B). According to deconvoluted CD data, both fibrils grown on the template and in the bulk solution were found to contain about 47% of cross β-sheet secondary structure, while cross β-sheet content in the ''fresh'' insulin solution was 25%. This suggests the transition of native insulin into amyloid form occurs at the template surface, which causes the formation of amyloid fibrils on the template as illustrated in Fig. 5. It is noteworthy that the conformational change of the amyloid-β monomer to neurotoxic amyloid was also mediated by interaction with plaques from the Alzheimer's disease patient (Esler et al., 2000).

Kinetics of Template-Directed Insulin Fibrillation

The kinetic mechanism of template-directed insulin fibrillation was studied using ThT-induced fluorescence. Previous study suggests that insulin forms amyloid fibrils via a nucleation–elongation mechanism in the solution (Brange et al., 1997; Nielsen et al., 2001). According to the model, the nucleation step is slow and unfavorable, while fibril elongation occurs rapidly with first-order fashion. The inset in Figure 6 shows that the deposition of the insulin monomer onto the template occurs with first-order kinetics without lag time. A similar result was reported for the growth of Alzheimer's amyloid-β plaques, which displayed first-order kinetics (Esler et al., 1996). When the effect of the soluble insulin monomer concentration on amyloid deposition was investigated, the fibril growth rate on the template increased

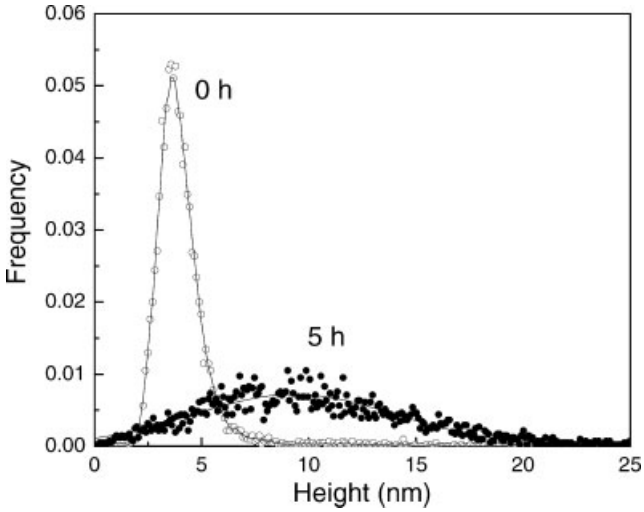

Figure 2. Height distribution of amyloid aggregates on the template at 0 and 5 h incubation. Gaussian curves were used to fit the distribution.

almost linearly at low insulin concentrations, but it tended toward saturation point at higher insulin concentrations (Fig. 6). Due to the difficulty in correlating ThT-induced fluorescence to actual fibril size (LeVine, 1993; Naiki and Nakakuki, 1996), the deposition constant of amyloid fibrils could not be evaluated quantitatively here, but the feature of the template-directed amyloid growth was similar to the Langmuir isotherm. In the case of amyloid growth on a solid template, the deposition of insulin monomers could occur only at seeded sites on the template surface, thus the fibril growth rate was initially concentration dependent, but it reached saturation at above the critical concentration of the insulin monomer.

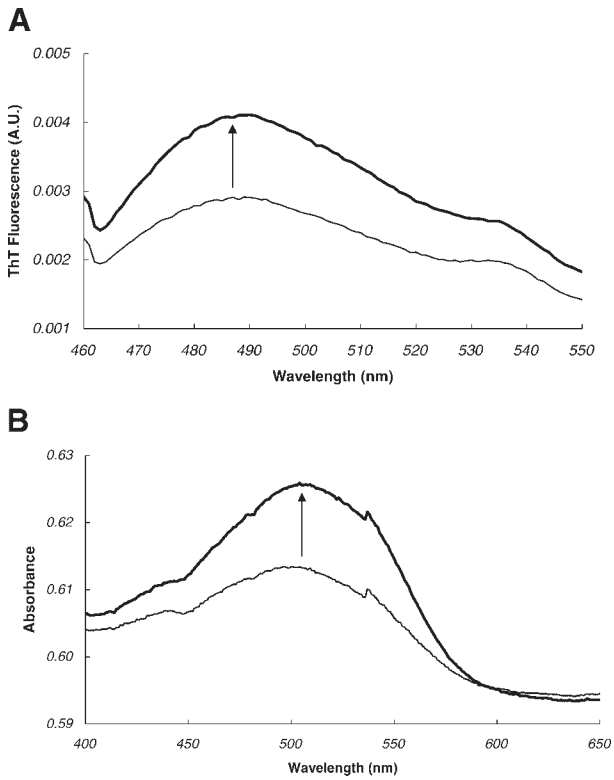

Figure 3. (**A**) Increase of ThT-induced fluorescence spectrum by the formation of amyloid fibrils on the template. (**B**) Increase of absorbance spectrum by birefringent Congo red binding to fibrils on the template. The synthetic amyloid template was incubated in (**A**) 1 mg/mL insulin solution and (**B**) 10 mg/mL insulin solution for 5 h for the measurement of spectral changes.

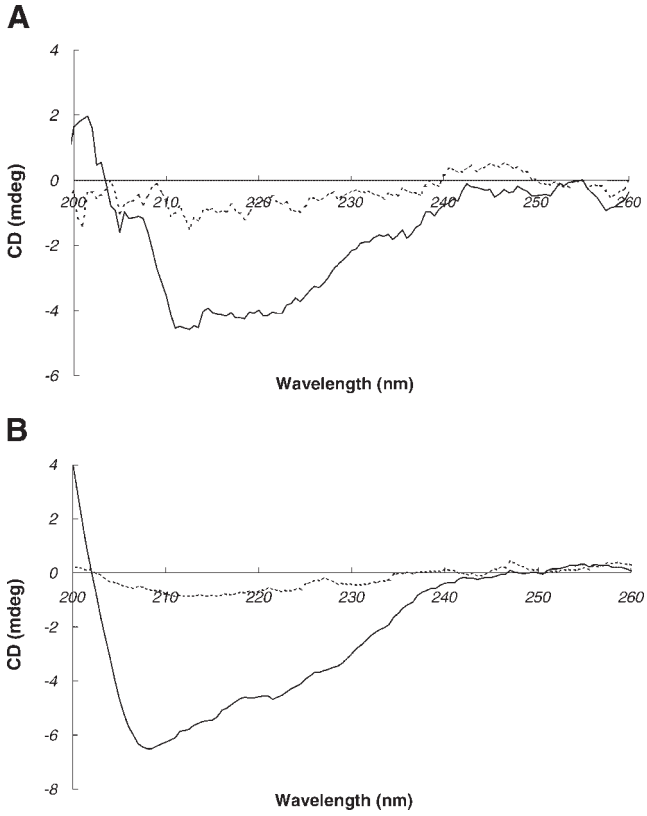

Figure 4. Changes of near-UV CD spectrum observed during the formation of insulin fibrils on the template and in the solution. Solid line: (**A**) CD spectrum for fresh insulin immobilized on the template and (**B**) CD spectrum for fresh insulin in the solution. Dotted line: (**A**) CD spectrum for insulin fibrils grown on the template for 6 h and (**B**) CD spectrum for insulin fibrils grown in a template-free solution for 16 h.

Application of Synthetic Template to Screening Inhibitors of Amyloid Deposition

Due to the possible relation of amyloid to pathology, many efforts had been made to screen compounds that interfere

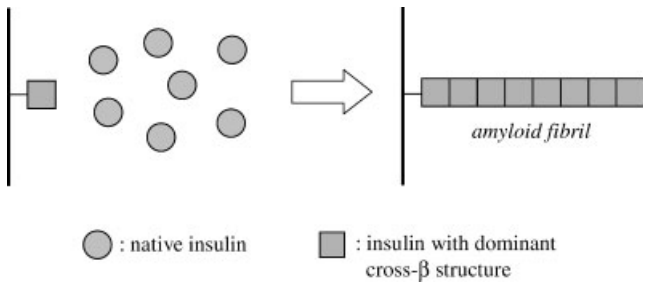

Figure 5. Schematic model showing a possible mechanism for template-directed deposition and growth of insulin amyloid fibrils.

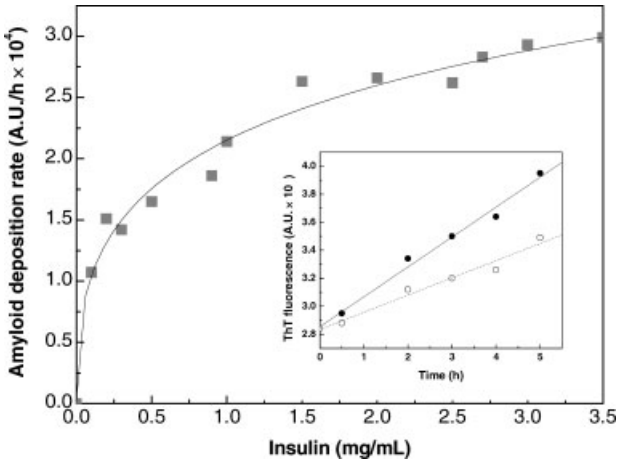

Figure 6. Effect of insulin concentration on amyloid deposition rate. The amyloid deposition rates were obtained by calculating the rate of ThT-induced fluorescence increase under various insulin concentrations. (**Inset**) Time profiles of ThT-induced fluorescence produced by amyloid formation on the template under different insulin concentrations in the solution: 0.3 mg/mL (○), 1 mg/mL (●).

with amyloid formation (Conway et al., 2001; Murphy, 2002; Tjernberg et al., 1996; Tomiyama et al., 1996). The synthetic amyloid template developed in this work can serve as an artificial template for high-throughput screening of amyloid deposition inhibitors in vitro. In order to demonstrate the possibility of using the template for screening inhibitors on amyloid deposition, several compatible solutes were tested. Compatible solutes, also known as chemical chaperones, had been found to accumulate in microorganisms under extreme environments preventing abnormal protein folding (Martins et al., 1997; Nunes et al., 1995; Santos and Da Costa, 2001). Among various compatible solutes, sucrose, maltose, trehalose and betaine were tested in this study to observe their effects on insulin amyloid deposition. The presence of those solutes had proved previously to be highly effective in preserving enzymatic activities against heating, freezing and drying (Borges et al., 2002; Lippert and Galinski, 1992; Santos and Da Costa, 2001). According to AFM images (Fig. 7), trehalose and betaine significantly suppressed amyloid formation on the template at 300 mM as indicated

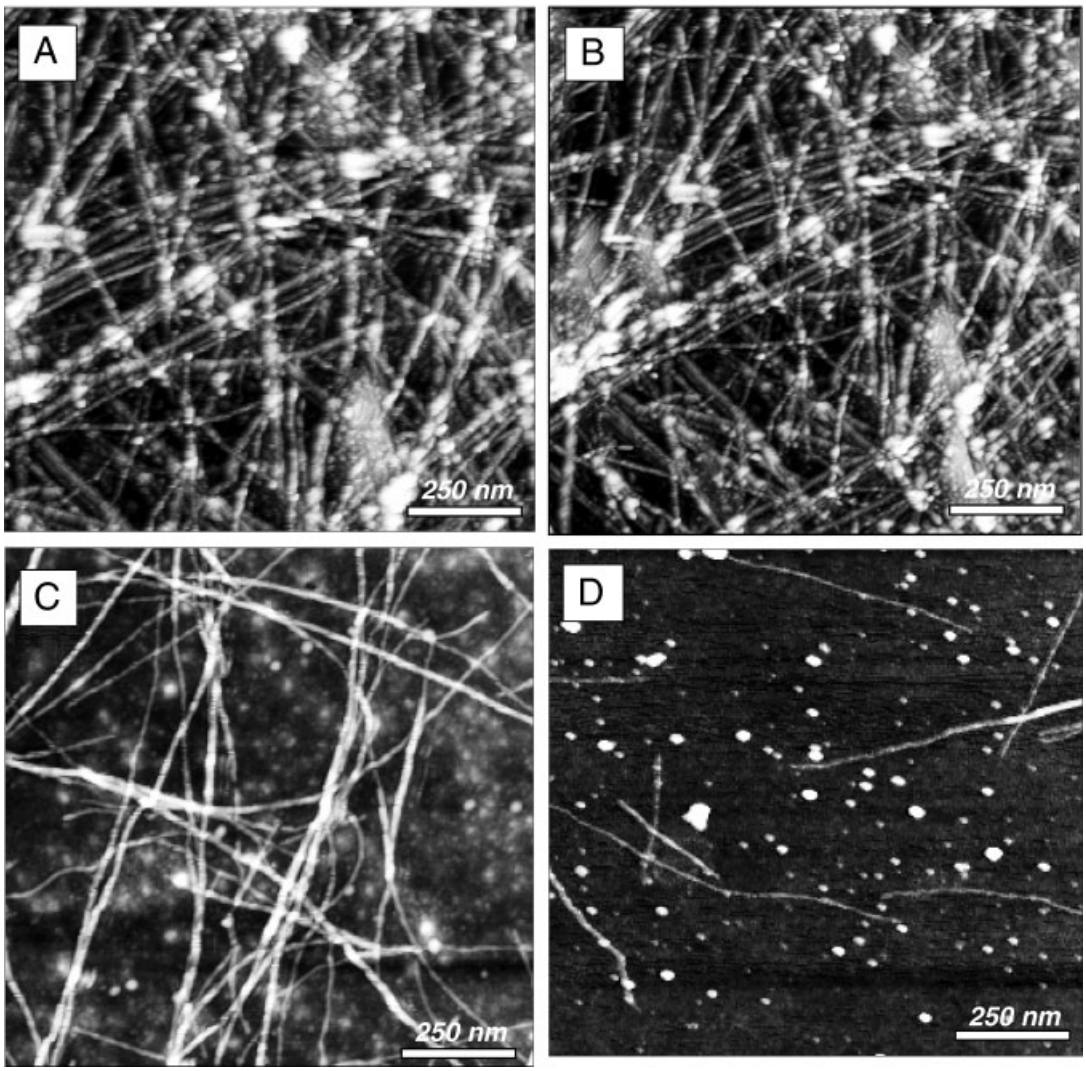

Figure 7. Effect of (**A**) sucrose, (**B**) maltose, (**C**) trehalose, and (**D**) betaine on insulin amyloid formation on a synthetic amyloid template. The template was incubated for 5 h in a solution containing fresh insulin (1 mg/mL) and each solute (300 mM), followed by direct observation using ex situ AFM.

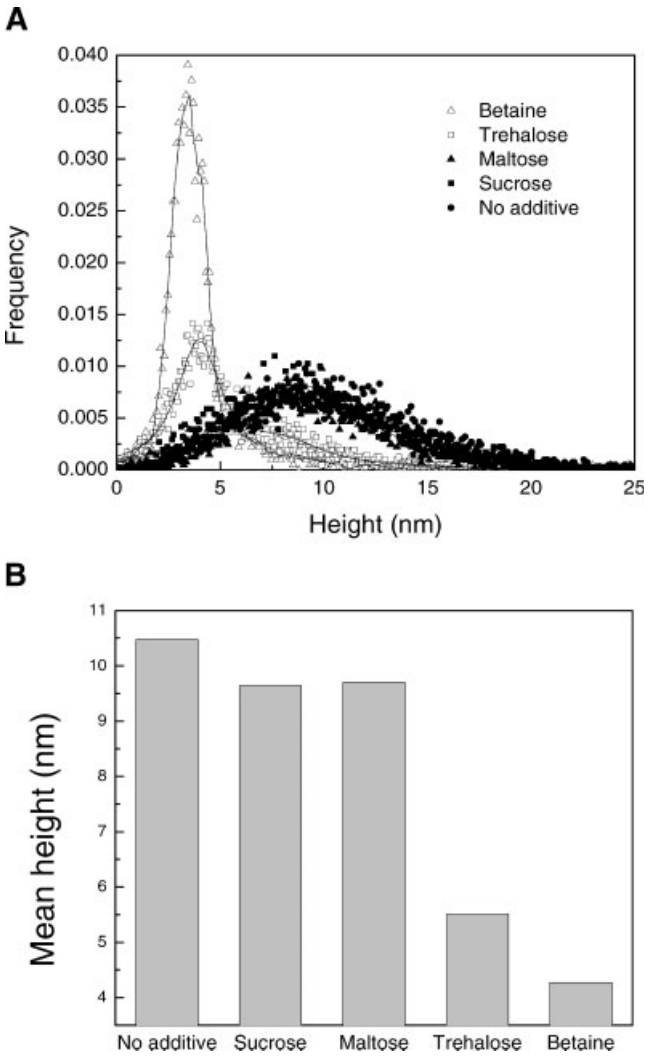

Figure 8. (**A**) Height distribution and (**B**) mean height of amyloid aggregates formed on the template after incubation in the absence (i.e., no additive) or in the presence of compatible solutes (300 mM) for 5 h.

by the low amounts of insulin fibrils on the template. In contrast, sucrose and maltose exhibited negligible inhibitory effect on amyloid deposition at the same concentration. Figure 8A shows the height distribution of amyloid aggregates on the template in the absence or presence of those compatible solutes. According to the result, betaine and trehalose significantly suppressed the shift of height distribution toward a higher magnitude. The comparison of mean aggregate heights also confirms the inhibitory effects of betaine and trehalose on insulin amyloid formation (Fig. 8B). According to a recent report (Tanaka et al., 2004), trehalose curbed Huntington's disease in mice by suppressing the formation of polyglutamine amyloid aggregates when administered orally as a 2% solution to transgenic mice. Among various disaccharides, trehalose showed the strongest inhibitory effect in the report. It needs to be seen why trehalose has a significantly different effect on amyloid formation than sucrose and maltose despite their structural similarities.

In this work, the properties and kinetics of template-directed insulin fibrillation were investigated using multiple analytical tools like AFM, ThT, CR, and CD, and the characteristics were found to be in agreement with previous studies performed with natural amyloid templates. Our observations showed that template-directed fibrillation was nucleation-independent and was accelerated by the interaction of insulin monomers with a seeded template. The fibril growth rate on the template followed saturation kinetics with respect to the insulin concentration in the solution. While identifying the most promising target compounds for preventing amyloid formation in clinical trials requires effective screening methods, our synthetic template can be a high-throughput screening tool for finding inhibitors of amyloid deposition in tissue. More than 20 kinds of amyloidogenic proteins have been reported so far, and some of them play central roles in the pathogenesis of amyloid diseases affecting millions of patients (Kisilevsky, 2000). Most amyloidogenic proteins, including insulin, had been known to follow a common amyloid formation pathway despite significant differences in their native structures (Harper and Lansbury, 1997; Murphy, 2002). The synthetic amyloid template developed in this work can be a useful model system for simulating fibrillization of amyloidogenic proteins in vivo.

References

Ahmad A, Millett IS, Doniach S, Uversky VN, Fink AL. 2003. Partially folded intermediates in insulin fibrillation. Biochemistry 42:11404–11416.

Borges N, Ramos A, Raven NDH, Sharp RJ, Santos H. 2002. Comparative study of the thermostabilizing properties of mannosylglycerate and other compatible solutes on model enzymes. Extremophiles 6:209–216.

Bouchard M, Zurdo J, Nettleton EJ, Dobson CM, Robinson CV. 2000. Formation of insulin amyloid fibrils followed by FTIR simultaneously with CD and electron microscopy. Protein Sci 9:1960–1967.

Brange J, Andersen L, Laursen ED, Meyn G, Rasmussen E. 1997. Toward understanding insulin fibrillation. J Pharm Sci 86:517–525.

Cohen FE, Prusiner SB. 1998. Pathologic conformations of prion proteins. Annu Rev Biochem 67:793–819.

Conway KA, Rochet J-C, Bieganski RM, Lansbury PT. 2001. Kinetic stabilization of the α-synuclein protofibril by a dopamine-α-synuclein adduct. Science 294:1346–1349.

Esler WP, Stimson ER, Ghilardi JR, Vinters HV, Lee JP, Mantyh PW, Maggio JE. 1996. In vitro growth of Alzheimer's disease β-amyloid plaques displays first-order kinetics. Biochemistry 35:749–757.

Esler WP, Stimson ER, Ghilardi JR, Felix AM, Lu Y-A, Vinters HV, Mantyh PW, Maggio JE. 1997. Aβ deposition inhibitor screen using synthetic amyloid. Nat Biotechnol 15:258–263.

Esler WP, Stimson ER, Mantyh PW, Maggio JE. 1999. Deposition of soluble amyloid-β onto amyloid templates: with application for the identification of amyloid fibril extension inhibitors. Methods Enzymol 309:350–374.

Esler WP, Stimson ER, Jennings JM, Vinters HV, Ghilardi JR, Lee JP, Mantyh PW, Maggio JE. 2000. Alzheimer's disease amyloid propagation by a template-dependent dock–lock mechanism. Biochemistry 39:6288–6295.

Fändrich M, Fletcher MA, Dobson CM. 2001. Amyloid fibrils from muscle myoglobin. Nature 410:165–166.

Harper JD, Lansbury PT. 1997. Models of amyloid seeding in Alzheimer's disease and scrapie: mechanistic truths and physiological consequences

of the time-dependent solubility of amyloid proteins. Annu Rev Biochem 66:385–407.

Jiménez JL, Nettleton EJ, Bouchard M, Robinson CV, Dobson CM, Saibil HR. 2002. The protofilament structure of insulin amyloid fibrils. Proc Natl Acad Sci USA 99:9196–9201.

Kisilevsky R. 2000. Review: amyloidogenesis—unquestioned answers and unanswered questions. J Struct Biol 130:99–108.

Kowalewski T, Holtzman DM. 1999. In situ atomic force microscopy study of Alzheimer's β-amyloid peptide on different substrates: new insights into mechanism of β-sheet formation. Proc Natl Acad Sci USA 96:3688–3693.

Lansbury PT. 1999. Evolution of amyloid: what normal protein folding may tell us about fibrillogenesis and disease. Proc Natl Acad Sci USA 96:3342–3344.

LeVine H. 1993. Thioflavin T interaction with synthetic Alzheimer's disease β-amyloid peptides: detection of amyloid aggregation in solution. Protein Sci 2:404–410.

Lippert K, Galinski EA. 1992. Enzyme stabilization by ectoine-type compatible solutes: protection against heating, freezing and drying. Appl Microbiol Biotechnol 37:61–65.

Lomakin A, Chung DS, Benedek GB, Kirschner DA, Teplow DB. 1996. On the nucleation and growth of amyloid β-protein fibrils: Detection of nuclei and quantitation of rate constants. Proc Natl Acad Sci USA 93:1125–1129.

Macario AJL, de Macario E. 2000. Stress and molecular chaperones in disease. Int J Clin Lab Res 30:49–66.

Martins LO, Huber R, Huber H, Stetter KO, Da Costa MS, Santos H. 1997. Organic solutes in hyperthermophilic Archaea. Appl Environ Microbiol 63:896–902.

McLaurin J, Yang D-S, Yip CM, Fraser PE. 2000. Review: modulating factors in amyloid-β fibril formation. J Struct Biol 130:259–270.

Murphy RM. 2002. Peptide aggregation in neurodegenerative disease. Annu Rev Biomed Eng 4:155–174.

Naiki H, Nakakuki K. 1996. First-order kinetic model of Alzheimer's β-amyloid fibril extension in vitro. Lab Invest 74:374–383.

Nielsen L, Khurana R, Coats A, Frokjaer S, Brange J, Vyas S, Uversky VN, Fink AL. 2001. Effect of environmental factors on the kinetics of insulin fibril formation: elucidation of the molecular mechanism. Biochemistry 40:6036–6046.

Nunes OC, Manaia CM, Da Costa MS, Santos H. 1995. Compatible solutes in the thermophilic bacteria *Rhodothermus marinus* and *Thermus thermophilus*. Appl Environ Microbiol 61:2351–2357.

Rochet J-C, Lansbury PT. 2000. Amyloid fibrillogenesis: themes and variations. Curr Opin Struct Biol 10:60–68.

Rymer DL, Good TA. 2000. The role of prion peptide structure and aggregation in toxicity and membrane binding. J Neurochem 75:2536–2545.

Santos H, Da Costa MS. 2001. Organic solutes from thermophiles and hyperthermophiles. Methods Enzymol 334:302–315.

Serpell LC. 2000. Alzheimer's amyloid fibrils: structure and assembly. Biochim Biophys Acta 1502:16–30.

Sharp JS, Forrest JA, Jones RAL. 2002. Surface denaturation and amyloid fibril formation of insulin at model lipid–water interfaces. Biochemistry 41:15810–15819.

Sipe JD, Cohen AS. 2000. Review: history of the amyloid fibril. J Struct Biol 130:88–98.

Slavotinek AM, Biesecker LG. 2001. Unfolding the role of chaperones and chaperonins in human disease. Trends Genet 17:528–535.

Tanaka M, Machida Y, Niu S, Ikeda T, Jana NR, Doi H, Kurosawa M, Nekooki M, Nukina N. 2004. Trehalose alleviates polyglutamine-mediated pathology in a mouse model of Huntington disease. Nature Med 10:148–154.

Thomas PJ, Qu B-H, Pedersen PL. 1995. Defective protein folding as a basis of human disease. Trends Biol Sci 20:456–459.

Tjernberg LO, Naslund J, Lindqvist F, Johansson J, Karlstrom AR, Thyberg J, Terenius L, Nordstedt C. 1996. Arrest of β-amyloid fibril formation by a pentapeptide ligand. J Biol Chem 271:8545–8548.

Tomiyama T, Shoji A, Kataoka K-I, Suwa Y, Asano S, Kaneko H, Endo N. 1996. Inhibition of amyloid beta protein aggregation and neurotoxicity by rifampicin. J Biol Chem 271:6839–6844.

Wang SS-S, Becerra-Arteaga A, Good TA. 2002. Development of a novel diffusion-based method to estimate the size of the aggregated Aβ species responsible for neurotoxicity. Biotechnol Bioeng 80:50–59.

Zhu M, Souillac PO, Ionescu-Zanetti C, Carter SA, Fink AL. 2002. Surface-catalyzed amyloid fibril formation. J Biol Chem 277:50914–50922.